

Application of the GIXRD Technique to Investigation of Damaged Layers in $\text{NaNd}(\text{WO}_4)_2$ and $\text{NaNd}(\text{MoO}_4)_2$ Ceramics Irradiated with High-Energy Ions

© P.A. Yunin,¹ A.A. Nazarov,^{1,2} E.A. Potanina²

¹Institute of Physics of Microstructures, Russian Academy of Sciences, 603087 Nizhny Novgorod, Russia

²Lobachevsky State University, 603022 Nizhny Novgorod, Russia
e-mail: yunin@ipmras.ru

Received March 30, 2022

Revised March 30, 2022

Accepted March 30, 2022

The technique of grazing incidence X-ray diffractometry (GIXRD) was used to study damaged layers in $\text{NaNd}(\text{WO}_4)_2$ and $\text{NaNd}(\text{MoO}_4)_2$ ceramics irradiated with high-energy ions. The possibilities and applicability limits of the technique for the analysis of such samples are shown. Estimates of the degree of amorphization in near-surface layers of ceramics are given depending on the irradiation dose. The higher resistance of $\text{NaNd}(\text{MoO}_4)_2$ ceramics to external radiation exposure as compared to $\text{NaNd}(\text{WO}_4)_2$ has been demonstrated.

Keywords: X-ray diffraction, Parallel beam method, Grazing incidence geometry, Ion irradiation, Ceramics, Radiation resistance, Amorphization, Damaged layer.

DOI: 10.21883/TP.2022.08.54556.69-22

Introduction

One of the main non-destructive methods of studying the crystal structure of solids is X-ray diffraction analysis. A special technique of X-ray diffraction analysis requiring the use of a parallel primary beam („parallel beam method“) is X-ray diffractometry in the geometry of grazing incidence (grazing incident x-ray diffractometry, GIXRD). The spread of multilayer X-ray optics of the primary beam has led to the widespread use of this technique not only on synchrotrons [1,2], but also on laboratory diffractometers [3]. An important feature of the method is that the angle of incidence of radiation on the sample throughout the experiment, in contrast to the „classical“ analysis in the Bragg–Brentano geometry remains unchanged. At the same time, the information depth of the analysis is determined by the photoelectronic absorption of X-ray radiation in the sample and the phenomenon of total external reflection (TER). Near the TER angle, the depth of penetration depends very sharply on the magnitude of the angle of grazing incidence α . Thus, varying the angle of incidence of X-ray radiation on a sample in the method of X-ray diffractometry in the geometry of sliding incidence makes it possible to control the effective information depth of diffraction analysis in the range from units of nanometers to units of microns. It becomes possible to analyze the distribution of crystal phases in depth, to investigate deformations and structural defects in the near-surface layers of [3–5]. Such analysis capabilities are becoming in demand in the diagnosis of thin polycrystalline films [6], as well as near-surface disturbed

layers in polycrystalline materials caused by the peculiarities of mechanical processing, ion etching and implantation or radiation exposure [7,8]. When solving the problem of searching for radiation-resistant materials, a diagnostic technique is required that allows obtaining quantitative estimates of the thickness of the disturbed layers and the degree of amorphization of crystalline phases in them caused by radiation exposure. This paper is devoted to the adaptation and application of the GIXRD technique for the analysis of disturbed layers in ceramics exposed to high-energy ions.

1. Experimental

Ceramics based on mineral-like compounds [9,10], including those with the structure of the mineral scheelite [11,12], are being studied as promising materials for the immobilization of components of radioactive waste. Isostructured scheelite-like compounds can contain many elements in their composition, the isotopes of which are present in the waste of radiochemical technologies [13,14]. In this paper, two series of ceramic samples $\text{NaNd}(\text{WO}_4)_2$ (NNW) and $\text{NaNd}(\text{MoO}_4)_2$ (NNMo) with the structure of the mineral scheelite [15–17] were studied. For the synthesis of such tungstates and molybdates, a method based on the precipitation reaction from solutions of metal salts was used. To obtain ceramics, the method of electropulse plasma sintering was used, which consists in high-speed heating of powder materials by passing successive DC pulses through the sintered material and graphite mold with simultaneous application of pressure [10,15–18]. The sintering process

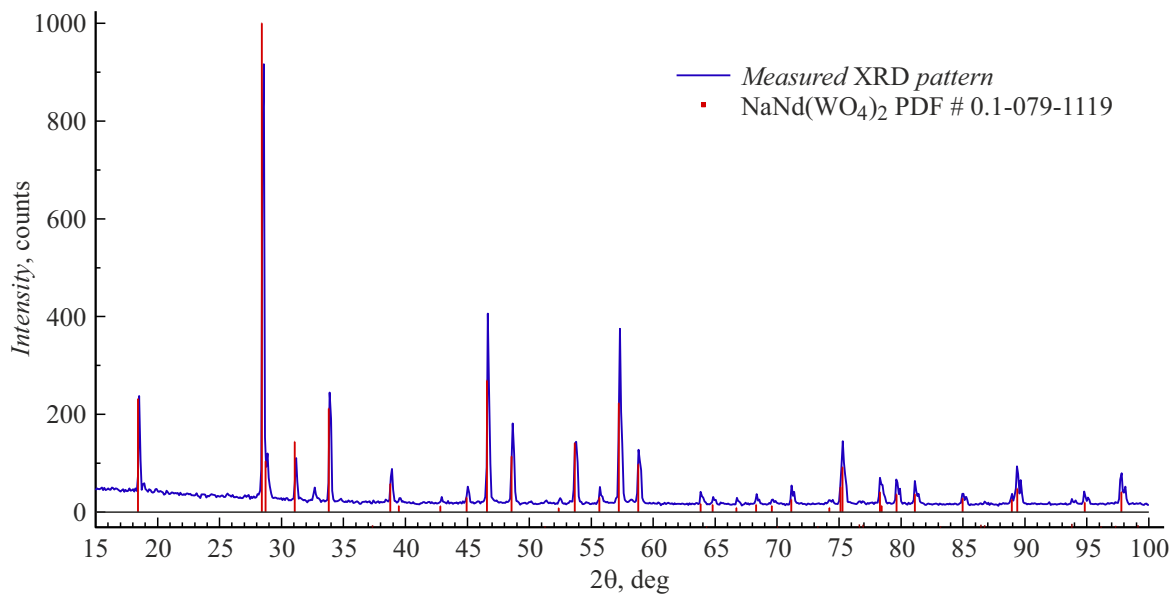


Figure 1. Diffractogram of the original NNW ceramics before irradiation, taken in symmetrical geometry.

was carried out on the DR installation. SINTER model SPS-625 Spark Plasma Sintering System (SPS SYNTEX INC. Ltd, Japan). As a result of sintering, cylindrical samples with a diameter of $d = 12$ mm and a thickness of $h = 2$ mm were obtained. To test the radiation resistance of ceramics, the samples were irradiated with heavy ions Ar ($E = 46$ MeV), Kr ($E = 107$ MeV) and Xe ($E = 160$ MeV) with four different doses of $6 \cdot 10^{10}$, $2 \cdot 10^{11}$, $6 \cdot 10^{11}$, $2 \cdot 10^{12}$ cm $^{-2}$, the temperature of the samples during irradiation did not exceed 50°C . This approach to the simulation of radiation exposure is traditionally used to assess the radiation resistance of materials, as it simulates the conditions of irradiation by fission products of nuclear fuel. It is known that the range of ions with the energies of fission fragments does not exceed $10\ \mu\text{m}$. In this case, radiation defects created by the electronic braking channel are formed in the near-surface layer of the material [19]. Such structural changes can be effectively investigated by X-ray diffractometry in the geometry of grazing incidence.

X-ray diffractometry in the geometry of grazing incidence was carried out on a Bruker D8 Discover laboratory X-ray diffractometer (vacuum X-ray tube, $\text{CuK}\alpha$ radiation) in the geometry of a parallel beam [20] with a parabolic Goebel mirror, a round collimator 1 mm on the primary beam and a slit Soller 0.2° in front of the detector. In each series of GIXRD experiments, the angle of incidence α of the primary beam per sample ranged from 1 to 10° , scanning in each experiment was carried out by a detector at angle 2θ . Before the GIXRD measurements, an X-ray diffraction experiment was performed in the „classical“ Bragg–Brentano geometry for non-irradiated samples.

2. Results and discussion

A characteristic view of the diffractogram taken in symmetrical geometry for the NNW ceramic sample is shown in Fig. 1. One crystal phase of $\text{NaNd}(\text{WO}_4)_2$ with a scheelite structure was registered in the sample. Similar results were obtained for ceramics of the NNMo series. Based on the obtained diffractograms, the most intense diffraction reflections of the (112) phases NNW and NNMo, located near the angle $2\theta = 28.3^\circ$, were selected for GIXRD analysis.

Then, for each sample exposed to different types of ions with different doses, a series of GIXRD experiments with different angles of incidence were performed α , varying in the limit from 1 to 10° . Typical experimental results for NNW ceramics before and after irradiation with Kr ions (107 MeV, $6 \cdot 10^{11}$ textcm $^{-2}$) are shown in Fig. 2.

The processing of the measurement results consisted in analyzing the dependence of the integral intensity of the diffraction peak on the angle of incidence α using theoretical calculations and a broken layer model in samples. The following expression was used to construct theoretical dependencies (1) [21]:

$$I(\alpha, 2\theta) = \int_0^h |T(\alpha, n)|^2 A(z, \alpha, 2\theta) G(\alpha, \Delta V) dz, \quad (1)$$

where $A(z, \alpha, 2\theta)$ — coefficient describing the absorption of an X-ray beam at a depth of z , $G(\alpha, \Delta V)$ — coefficient taking into account the geometric and other characteristics of the sample, h — sample thickness (taken as infinity due to the smallness of the penetration depth of the X-ray beam compared to the thickness of the sample), α — angle of incidence, $T(\alpha)$ — Fresnel radiation penetration coefficient

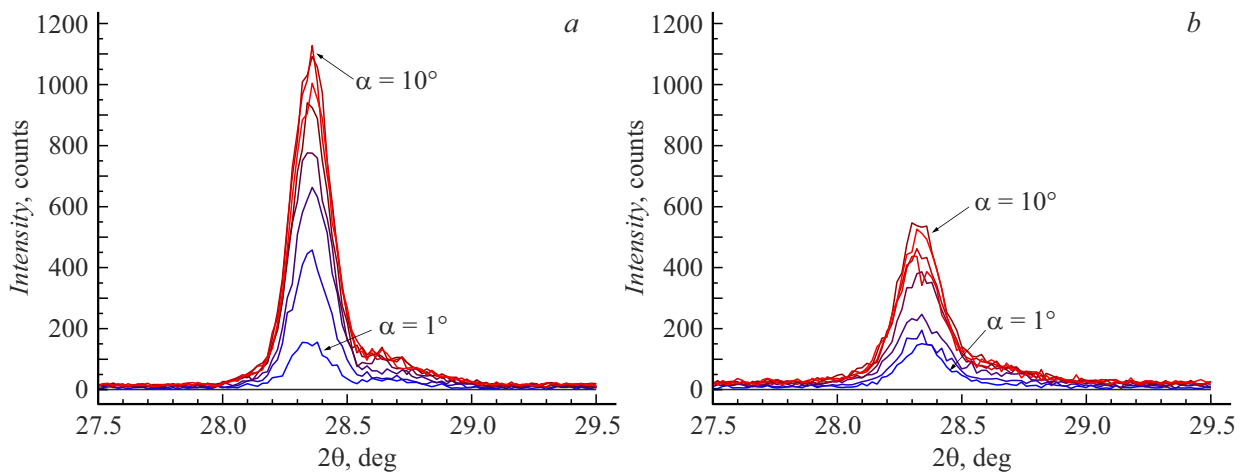


Figure 2. Results of X-ray diffraction GIXRD analysis of NNW ceramics at angles of incidence α from 1 to 10°: *a* — 2θ -reflection scans (112) of the original sample; *b* — similar scans for ceramics exposed to irradiation ions Kr (107 MeV, $6 \cdot 10^{11} \text{ cm}^{-2}$).

Table 1. The degree of amorphization of the near-surface layer for a series of NNMo and NNW ceramics exposed to different doses of Kr ions ($E = 107 \text{ MeV}$)

Fluence, cm^{-2}	Degree of amorphization of the near-surface layer, %	
	NNMo	NNW
$6 \cdot 10^{10}$	25 ± 5	23 ± 5
$2 \cdot 10^{11}$	37 ± 5	45 ± 5
$6 \cdot 10^{11}$	40 ± 5	57 ± 5
$2 \cdot 10^{12}$	48 ± 5	72 ± 5

into the film, refractive index $n = 1 - \delta + i\beta$, where (δ, β) — dispersion and absorption corrections specific to a particular material [22]. In our case, the coefficient $G(\alpha, \Delta V)$ includes a model of an amorphized layer near the surface. The desired parameters of the model are the degree of amorphization and thickness. The remaining parameters determining the geometry of the experiment and the sample material in the case of NNW ceramics were fixed: the length of the sample in the diffraction plane $L = 12 \text{ mm}$, the width of the slit on the primary beam $w = 1 \text{ mm}$, $\delta = 9.55 \cdot 10^{-6}$, $\beta = 7.67 \cdot 10^{-7}$.

Fig. 3 shows the characteristic results of processing experimental data, together with the adjusted theoretical dependence in the case of NNW ceramics irradiated with Kr (107 MeV, $6 \cdot 10^{11} \text{ cm}^{-2}$) and initial.

The differences between the dependencies for non-irradiated and irradiated ceramics could be described by changing only one parameter — intensity multiplier. For the results shown in Fig. 3, *b*, its value was 0.57 compared to non-irradiated ceramics. The decrease in intensity was interpreted as „amorphization“ of the near-surface layer of irradiated ceramics, and the value itself was defined

Table 2. The value of the depth of the disturbed layer calculated in SRIM for NNMo and NNW ceramics irradiated with ions of different energies

Type of ions and their energy	Ion penetration depth, μm	
	NNMo	NNW
Ar ($E = 46 \text{ MeV}$)	8.7	8.3
Kr ($E = 107 \text{ MeV}$)	11.3	10.8
Xe ($E = 160 \text{ MeV}$)	11.7	11.1

as „degree of amorphization“, integrally characterizing the violation of crystallinity in the irradiated sample. There was no change in the type of dependence on the angle of incidence, which suggests the homogeneity of the amorphization of the crystalline phase in depth within the depth range of the analysis. The estimate of the information depth of X-ray penetration into the NNW sample is $2 \mu\text{m}$ at an angle of incidence of 10° [22]. This allows us to give an experimental estimate of the thickness of the disturbed layer in these samples $> 2 \mu\text{m}$. Processing of the entire array of experimental data showed an increase in the degree of amorphization with an increase in the radiation dose from 20% at a dose of $6 \cdot 10^{10}$ for NNMo ceramics to 70% at a dose of $2 \cdot 10^{12}$ for ceramics NNW. NNMo ceramics have shown greater resistance of the crystalline phase to external radiation compared with NNW at the same radiation doses. The formation of new crystalline phases in the irradiated samples was not observed. Estimates of the degree of amorphization for each of the ceramics when irradiated with Kr ions ($E = 107 \text{ MeV}$) are given in Table 1.

In addition to the X-ray diffraction experiment, the ion implantation process was simulated for each series of ceramics in the SRIM [23,24] software package. As a result

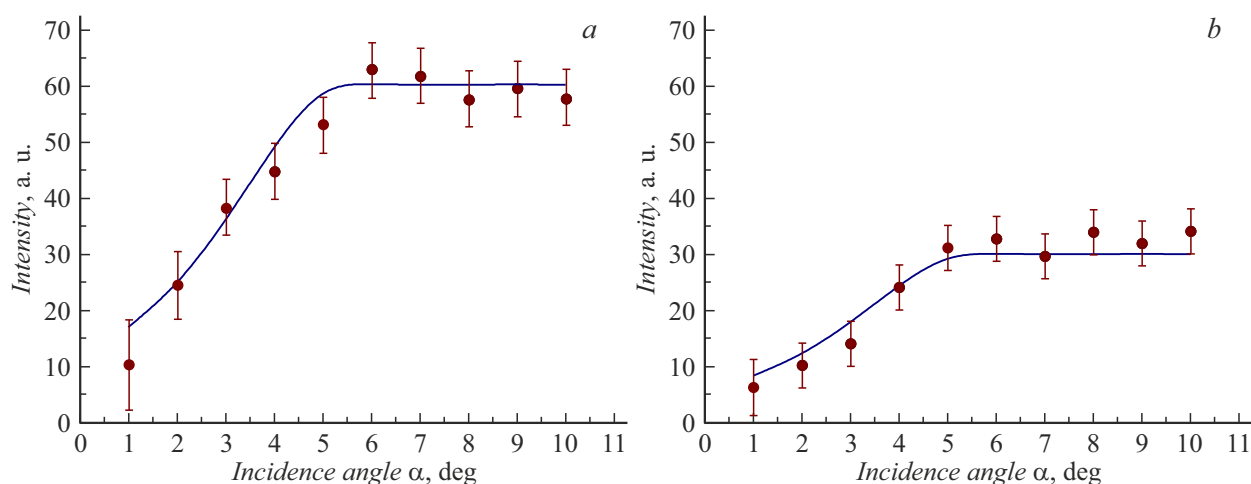


Figure 3. Dependences of the reflection intensity (112) of the NW phase on the angle of incidence α : *a* — for non-irradiated ceramics; *b* — for irradiated ceramics (Kr, 107 MeV, $6 \cdot 10^{11} \text{ cm}^{-2}$). Experiment and calculation.

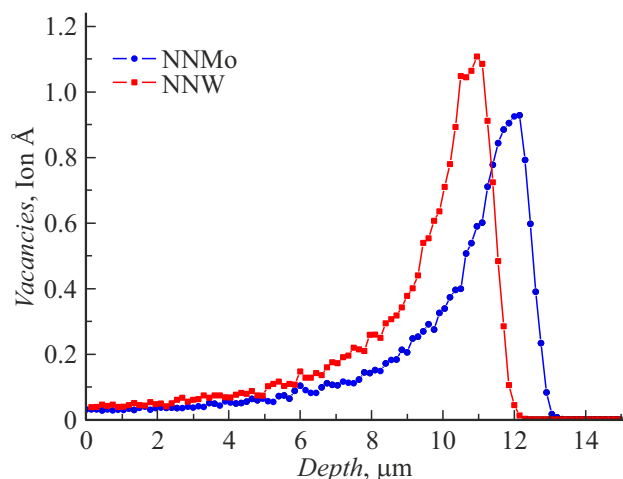


Figure 4. The result of modeling in SRIM the density of the depth distribution of vacancies caused by the action of primary ions and recoil atoms for NNMo and NNW materials irradiated with Kr ions ($E = 107 \text{ MeV}$).

of the simulation, estimates of the penetration depths of ions into NNM and NNMo materials were made, the results are given in Table 2. The result of SRIM simulation of the density of the depth distribution of vacancies caused by the action of primary ions and recoil atoms for NNMo and NNW materials irradiated with Kr ions ($E = 107 \text{ MeV}$) is shown in Fig. 4.

The estimation of the thickness of the disturbed layers turned out to be greater than the depth of penetration of X-ray radiation into the samples ($2 \mu\text{m}$) in our series of experiments. The conducted modeling (Fig. 4) qualitatively confirms the relatively homogeneous distribution of the defect concentration within the investigated depth range and does not contradict the experimental results obtained.

Conclusion

The GIXRD analysis technique was adapted to diagnose disturbed layers in polycrystalline ceramics NNMo and NNW irradiated with high-energy ions. Estimates of the degree of amorphization in the near-surface layers of ceramics depending on the radiation dose are given. The greater resistance of the near-surface layers of NNMo ceramics to external radiation exposure compared with NNW at the same radiation doses has been experimentally demonstrated. The experimental results do not contradict the estimates made by modeling the ion implantation process in the SRIM software package.

Acknowledgments

Radiation tests of ceramics samples $\text{NaNd}(\text{WO}_4)_2$, $\text{NaNd}(\text{MoO}_4)_2$ were carried out on the cyclotron IC-100 of the Laboratory of Nuclear Reactions of the Joint Institute for Nuclear Research, Dubna city. The ceramics were obtained in the Laboratory of Ceramics Technology of the Scientific Research Institute of Physics and Technology of the NNGU. For the research, the Common Use Center (CUC) equipment of the IFM RAS „Physics and Technology of micro- and nanostructures“ was used.

Funding

The study was carried out with the financial support of the RFBR as part of the scientific project №20-21-00145_Rosatom. X-ray diffraction studies of samples before and after irradiation were performed in the laboratory for the diagnosis of radiation defects in solid-state nanostructures of the IFM RAS with the support of the Ministry of Science and Higher Education of the Russian Federation (g/z № 0030-2021-0030).

Conflict of interest

The authors declare that they have no conflict of interest.

References

- [1] H. Dosch, B.W. Batterman, D.C. Wack. *Phys. Rev. Lett.*, **56**, 1144–1147 (1986). DOI: 10.1103/PhysRevLett.56.1144
- [2] M.F. Doerner, S. Brennan. *J. Appl. Phys.*, **63**, 126–131 (1988). DOI: 10.1063/1.340503
- [3] P. Colombi, P. Zanola, E. Bontempi, R. Roberti, M. Gelfi, L.E. Depero. *J. Appl. Crystallogr.*, **39**, 176–179 (2006). DOI: 10.1107/s0021889805042779
- [4] P.F. Fewster, N.L. Andrew, V. Holy, K. Barmak. *Phys. Rev. B*, **72**, 174105 (2005). DOI: 10.1103/PhysRevB.72.174105
- [5] M.F. Toney, S. Brennan. *J. Appl. Phys.*, **65**, 4763–4768 (1989). DOI: 10.1063/1.343230
- [6] P.A. Yunin, Yu.N. Drozdov, N.S. Gusev. *Poverkhnost'. Rentgen., sin-khrotron. i nejtron. issled.* **7**, 74–77 (in Russian). DOI: 10.7868/S0207352818070119
- [7] S. Bera, B. Satpati, D.K. Goswami, K. Bhattacharjee, P.V. Satyam, B.N. Dev. *J. Appl. Phys.*, **99**, 074301 (2006). DOI: 10.1063/1.2184429
- [8] A.J. London, B.K. Panigrahi, C.C. Tang, C. Murray, C.R.M. Grovenor. *Scripta Mater.*, **110**, 24–27 (2016). DOI: 10.1016/j.scriptamat.2015.07.037
- [9] C.M. Jantzen, W.E. Lee, M.I. Ojovan. *Radioactive Waste Management and Contaminated Site Clean-Up. Processes, Technologies and International Experience* (Woodhead Published Limited, Oxford, Cambridge, Philadelphia, New Delhi, 2013), ch. 6, p. 171. DOI: 10.1533/9780857097446.1.171
- [10] A.I. Orlova. *J. Nucl. Mater.*, **559**, 153407 (2022). DOI: 10.1016/j.jnucmat.2021.153407
- [11] G. Canu, V. Buscaglia, C. Ferrara, P. Mustarelli, S. Gonçalves Patrício, A.I. Batista Rondão, C. Tealdi, F.M.B. Marques. *J. Alloys Compd.*, **697**, 392–400 (2017). DOI: 10.1016/j.jallcom.2016.12.111
- [12] J. Cheng, J. He. *Mater. Lett.*, **209**, 525–527 (2017). DOI: 10.1016/j.matlet.2017.08.094
- [13] D. Errandonea, F.J. Manjón. *Prog. Mater. Sci.*, **53**, 711–773 (2008). DOI: 10.1016/j.pmatsci.2008.02.001
- [14] R.H. Damascena dos Passos, M. Arab, C. Pereira de Souza, C. Leroux. *Cryst. Eng. Mater.*, **73**, 466–473 (2017). DOI: 10.1107/S2052520617002827
- [15] E.A. Potanina, A.I. Orlova, D.A. Mikhailov, A.V. Nokhrin, V.N. Chuvil'deev, M.S. Boldin, N.V. Sakharov, E.A. Lantsev, M.G. Tokarev, A.A. Murashov. *J. Alloys Compd.*, **774**, 182–190 (2019). DOI: 10.1016/j.jallcom.2018.09.348
- [16] E.A. Potanina, A.I. Orlova, A.V. Nokhrin, D.A. Mikhailov, M.S. Boldin, N.V. Sakharov, O.A. Belkin, E.A. Lantsev, M.G. Tokarev, V.N. Chuvil'deev. *Russ. J. Inorg. Chem.*, **64**, 296–302 (2019). DOI: 10.1134/S0036023619030161
- [17] M.G. Tokarev, E.A. Potanina, A.I. Orlova, S.A. Khainakov, M.S. Boldin, E.A. Lantsev, N.V. Sakharov, A.A. Murashov, S. Garcia-Granda, A.V. Nokhrin, V.N. Chuvil'deev. *Inorg. Mater.*, **55**, 730–736 (2019). DOI: 10.1134/S0020168519070203
- [18] M. Tokita. *Ceramics*, **4**, 160–198 (2021). DOI: 10.3390/ceramics4020014
- [19] F.F. Komarov, *UFN*, **187** (5), 465 (2017). DOI: 10.3367/UFNr.2016.10.038012
- [20] M. Birkholz. *Thin Film Analysis by X-Ray Scattering* (WILEY-VCH Verlag GmbH & Co. KGaA, Weinheim, 2006), p. 143–169.
- [21] P. Colombi, P. Zanola, E. Bontempi, L.E. Depero. *Spectrochim. Acta B*, **62**, 554–557 (2007). DOI: 10.1107/S0021889805042779
- [22] B.L. Henke, E.M. Gullikson, J.C. Davis. *Atom. Data Nucl. Data*, **54** (2), 181–342 (1993). DOI: 10.1006/adnd.1993.1013
- [23] J.F. Ziegler, J.P. Biersack, U. Littmark. *The Stopping and Range of Ions in Solids* (Pergamon Press, NY., 1984)
- [24] R.E. Stoller, M.B. Toloczko, G.S. Was, A.G. Certain, S. Dwaraknath, F.A. Garner. *Nucl. Instrum. Meth. B*, **310**, 75–80 (2013). DOI: 10.1016/j.nimb.2013.05.008